Journal of Nuclear Materials 386–388 (2009) 169–172

Contents lists available at ScienceDirect

Journal of Nuclear Materials

journal homepage: www.elsevier.com/locate/jnucmat

Positron annihilation of vacancy-type defects in neutron-irradiated 4H–SiC

Q. Xu, T. Yoshiie *, M. Okada

Research Reactor Institute, Kyoto University, Osaka 590-0494, Japan

ARTICLE INFO

PACS:
61.72.Ji
61.72.Cc
61.80.Fe
61.80.Hg
61.82.Fk

ABSTRACT

Annealing behavior of vacancy-type defects in n-type 4H–SiC, which was irradiated with neutrons up to a dose of 3.2×10^{21} m^{-2} ($E > 1$ MeV) at 20 °C, was investigated by positron annihilation spectroscopy. Isochronal annealing results indicate that there are four different recovery stages in the irradiated 4H–SiC. In stage I, in the temperature range of 20–100 °C, the defect recovery is attributed to recombination between close vacancies and interstitials, and carbon and silicon clusters are formed by the migration of their interstitials. In stage II (200–1100 °C), carbon and silicon interstitials disappear at permanent sinks due to the long-range migration. Silicon and carbon vacancies move actively in stage III (1200–1400 °C). In stage IV (>1400 °C), more stable silicon vacancy complexes dissociate. Although, no vacancy-type defects are observed in 4H–SiC after annealing at 1600 °C, interstitial-type or anti-site defects are stable.

© 2009 Elsevier B.V. All rights reserved.

1. Introduction

Silicon carbide (SiC) exhibits outstanding physical, chemical and electronic properties, such as higher blocking voltages, lower power losses, increased switching frequencies and high operational temperatures, all of which render SiC semiconductor devices suitable for operation in high-temperature, high-irradiation environments [1]. Furthermore, owing to its small cross-section, low activation, high-temperature strength and high thermal conductivity under neutron irradiation it can potentially be used in fusion systems [2]. It is well known that intrinsic defects and impurities often affect the electrical, optical and other physical properties of SiC. The annealing properties of intrinsic and impurity-related defects have been investigated in irradiated SiC by various experimental techniques, such as electron paramagnetic resonance (EPR) spectroscopy [3], deep level transient spectroscopy (DLTS) [4], photoluminescence spectroscopy (PL) [5], and positron annihilation spectroscopy (PAS) [4]. EPR and PAS are powerful tools to study vacancy-type defects, and DLTS and PL to study interstitial-type defects. Besides interstitials and vacancies of silicon and carbon, anti-site defects are induced by irradiation. Intrinsic defect migrations have been studied in great detail, not only by experiments, but also computer simulations. However, defect migration processes and the formation mechanism of defect clusters are still not well understood.

As mentioned above, PAS is a powerful tool to detect vacancy-type defects in condensed matter [6]. Doppler broadening of positron annihilation radiation can provide useful information about the element distribution around the annihilation site. Recently, Doppler broadening measurements were improved by a two-Ge-detector coincidence system, which decreased the background of high momentum contributions by about two or three orders of magnitude compared with traditional measurements using one Ge detector [7]. Coincidence Doppler broadening (CDB) has been used widely to detect precipitates in alloys [8–11]. Thus, in this work, the positron lifetime and coincidence Doppler broadening were used to measure the defects and segregation of elements in neutron-irradiated 4H–SiC.

2. Experimental procedure

A single crystal of n-type 4H–SiC manufactured by Nippon Steel Corporation was used in this work. The nitrogen concentration was about $1 \times 10^{17}/cm^3$. The specimens were sliced perpendicularly to the *c*-axis and both surfaces were polished with diamond powder. The samples were irradiated at 20 °C using the low-temperature irradiation facility of the Kyoto University Research Reactor with a neutron fluence of $3.2 \times 10^{21}/m^2$ ($E > 1$ MeV). Isochronal annealing was carried out from 50 °C to 1600 °C in a helium gas flow of about 1 l/min. Each temperature was maintained for 5 min. The recovery of defects was examined by positron lifetime measurements and coincidence Doppler broadening (CDB) measurements at room temperature (RT). The positron lifetime spectrometer had a time resolution of 190 ps (full width at half maximum) and each spectrum was accumulated to a total of over 2×10^6 counts. Doppler-broadening spectra were accumulated to a total of over 2×10^7 counts. The energy resolution was 1.4 keV at 551 keV.

* Corresponding author.
E-mail address: yoshiie@rri.kyoto-u.ac.jp (T. Yoshiie).

0022-3115/$ - see front matter © 2009 Elsevier B.V. All rights reserved.
doi:10.1016/j.jnucmat.2008.12.326

3. Results and discussion

The lifetime of unirradiated 4H–SiC was 136.2 ± 0.4 ps lower than the 151 ps reported by Puff et al. [12], who obtained their single-crystalline SiC wafers from Cree Research Inc. Vacancy-type defects were present in the matrix of these wafers before irradiation. By contrast, our 4H–SiC samples contained no vacancy defects before irradiation since two-lifetime-component analysis could not be carried out. Fig. 1 shows the changes in positron lifetime and intensity of the long lifetime τ_2 in 4H–SiC during isochronal annealing after neutron irradiation at 20 °C. τ_m is the positron mean lifetime. The short lifetime τ_1 mainly comes from annihilation of free positrons in the matrix, and the long lifetime τ_2 results from positron annihilation at defects such as vacancies or vacancy clusters. If vacancy-type defects exist in the matrix, τ_1 is less than the bulk lifetime τ_B, since $\tau_1 = 1/(\tau_B^{-1} + \kappa)$, where the net positron trapping rate $\kappa = I_2/I_1(\tau_B^{-1} - \tau_2^{-1})$. After irradiation, the long lifetime was 205.0 ± 3.4 ps, which was shorter than that of the $V_{Si}V_C$ di-vacancy (214 ps) and longer than that of the V_{Si} mono-vacancy (192–194 ps) [13]. Electron-paramagnetic-resonance (EPR) and electron-spin-echo (ESE) studies have revealed that isolated V_{Si}^-, V_{Si}^0 and V_C vacancies were formed under neutron irradiation at room temperature [14]. Thus, besides the mono-vacancies V_C and V_{Si}, $V_{Si}V_C$ di-vacancies were induced in this work. Although the long lifetime of 205 ps was the weighted average for the mono-vacancies V_{Si}, V_C and the $V_{Si}V_C$ di-vacancy, it mainly came from silicon vacancies since carbon vacancies did not trap positrons in 4H–SiC [15]. The changes of lifetime and intensity of long lifetime indicate that there are four recovery stages, stage I (20–100 °C), stage II (200–1100 °C), stage III (1200–1400 °C) and stage IV (>1400 °C), during isochronal annealing. The long lifetime and its density decrease in stages I, IV and III, respectively, but they do not change in stage II. The discussion below compares the lifetime results of isochronal annealing with the CDB results.

Fig. 2 shows typical ratio curves of irradiated 4H–SiC and annealed 4H–SiC to unirradiated 4H–SiC as a function of P_L, the electron-positron momentum in the direction of gamma emission

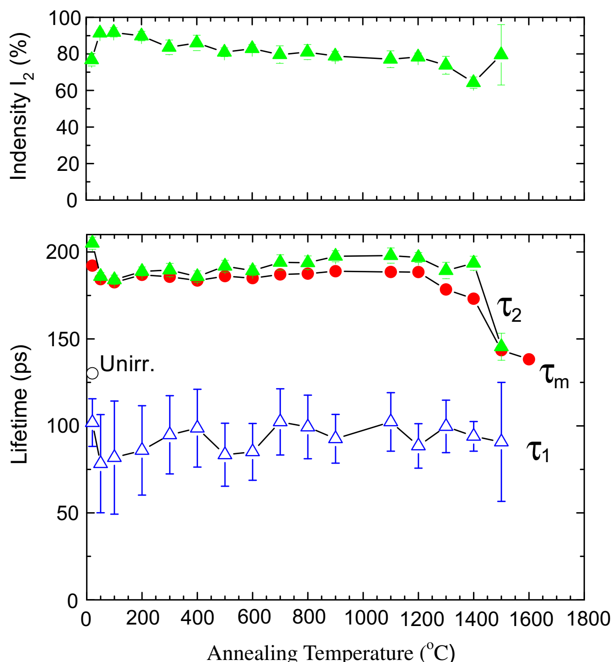

Fig. 1. Positron lifetime and intensity of long lifetime τ_2 of neutron-irradiated 4H–SiC during isochronal annealing.

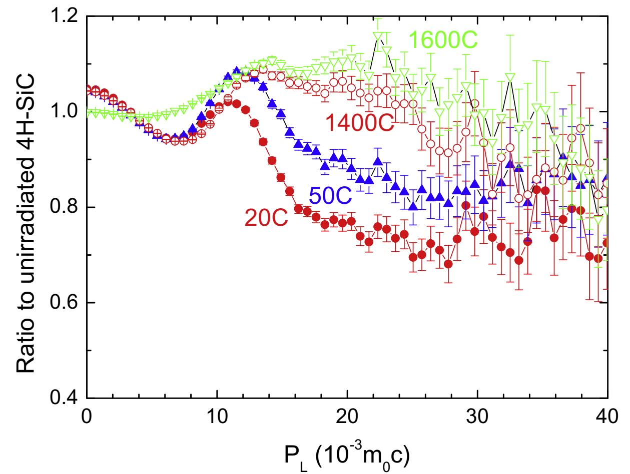

Fig. 2. Typical ratio curves of neutron-irradiated and annealed 4H–SiC to unirradiated 4H–SiC.

obtained from CDB [8]. After irradiation, the ratio curve was higher than 1 in the low-momentum region because more positrons were annihilated with valence electrons at the vacancies in irradiated 4H–SiC. During isochronal annealing from 50 °C to 1400 °C, the changes of the ratio curves in the low-momentum region were not prominent. However, upon annealing at 1600 °C, the ratio curve became flat, which meant that there were no vacancies in the 4H–SiC sample. This agrees with the lifetime results shown in Fig. 1, where two-lifetime-component analysis could not be carried out. In addition, the ratio curves show a peak near electron momentum $|P_L| = 1 \times 10^{-2}\ m_0c$, where c is the speed of light, and m_0 the static electron mass. The peak, which will be discussed below, disappeared after annealing at 1600 °C, and the electron momentum in the higher momentum region ($|P_L| > 2 \times 10^{-2}\ m_0c$) increased. In order to elucidate the recovery behavior of defects, the CDB spectra of 4H–SiC were compared with those of unirradiated carbon and silicon. In the case of unirradiated 4H–SiC, the silicon peak appears in the high momentum region of $|P_L| = 1.9 \times 10^{-2}\ m_0c$, and carbon peaks at $|P_L| = 1 \times 10^{-2}\ m_0c$ because the positrons are annihilated with both Si and C in 4H–SiC. For the irradiation at 20 °C, the ratio curves did not show a prominent silicon peak, but showed a prominent carbon peak. The CDB results indicated that the positrons were mainly trapped at silicon vacancies, which agreed with the lifetime results, since the electron momentum in the higher-momentum region came from the core electron of carbon around silicon vacancies. Upon annealing at 50 °C, however, not only the carbon peak, but also the silicon peak intensified. To investigate the mechanism of defect recovery during isochronal annealing, this study introduced the parameters S and W to estimate the amount of positrons annihilated with valence and core electrons, respectively. There are two types of core electrons in 4H–SiC: the core electrons of carbon and silicon. Here, S represents $|P_L|$ values in the range from 0 to $4 \times 10^{-3}\ m_0c$, while the W parameters for carbon and silicon core electrons, W_C and W_{Si}, respectively, correspond to $|P_L|$ values in the 8–12 $\times 10^{-3}\ m_0c$ and 17.5–22.5 $\times 10^{-3}\ m_0c$ range, respectively. Figs. 3 and 4 plot S–W_C and S–W_{Si}, respectively, and include the data for unirradiated 4H–SiC. In stage I (20–100 °C), both W_C and W_{Si} increased, but S decreased. On the basis of the comparison with lifetime results (Fig. 1), where the long lifetime τ_2 also decreased from 205.0 ps to 185.9 ps but its intensity increased from 76.8% to 91.4%, it is concluded that the size of the $V_{Si}V_C$ di-vacancy decreased and the proportion of positrons that were annihilated with vacancies increased due to the short-range mutual recombination

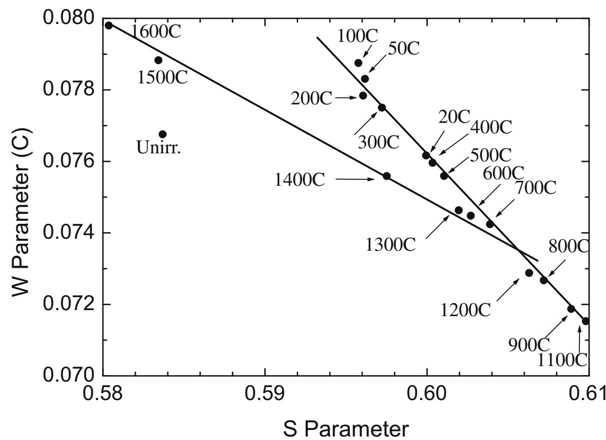

Fig. 3. Isochronal annealing behavior of the S–W_C plot.

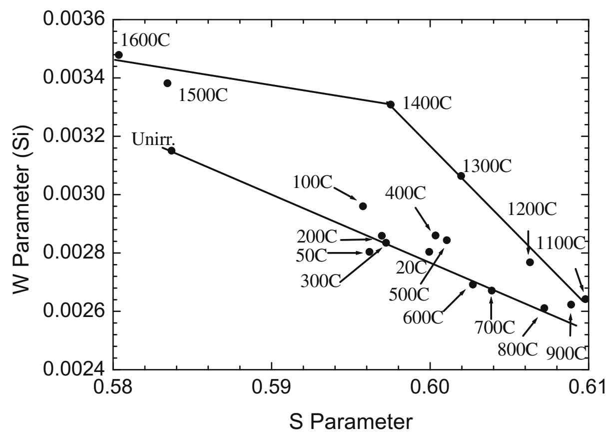

Fig. 4. Isochronal annealing behavior of the S–W_{Si} plot.

of Frenkel pairs [16,17]. Molecular dynamics (MD) simulations showed that the activation energies for defect recombination processes ranged from 0.22 to 1.6 eV for carbon Frenkel pairs and from 0.28 to 0.9 eV for silicon Frenkel pairs [18]. Carbon and silicon interstitials are mobile and recombine with vacancies by short-range migration even at temperatures below room temperature. The decrease in S during stage I was caused by the recombination of interstitials and vacancies. This also decreased the long lifetime. In addition, small clusters of carbon and silicon interstitials were possibly formed during their migration, which would have increased W_C and W_{Si}. In stage II (200–1100 °C), S increased and W_C decreased, while at the same time W_{Si} decreased, although, this decrease was not prominent. In this temperature region, the carbon and silicon interstitials migrated over a long range and disappeared at permanent sinks, such as surface of specimens, which decreased W_C and W_{Si} but did not change the long lifetime. The recovery processes of defects in stage III (1200–1400 °C) were relatively simple compared with those of stages I and II. Silicon and carbon vacancies became mobile and disappeared at sinks in this temperature region [19]. Thus, S decreased and W_C and W_{Si} increased due to the decrease of the proportion of positrons that were annihilated by vacancies with increasing annealing temperature. The lifetime results, where the long lifetime τ_2 did not change but its intensity decreased, also agreed with the disappearance at the sinks of mobile silicon vacancies. In stage IV (>1400 °C), S decreased, while W_C and W_{Si} increased. In stage III, mobile silicon vacancies were presumably trapped by nitrogen atoms to form $V_{Si}N_C$ complexes. Girka et al. reported that complexes of silicon vacancies and nitrogen atoms were annealed out around 1400 °C [20], although, some papers reported that $V_{Si}N_C$ is stable at temperature higher than 1400 °C [21]. The long lifetime τ_2 also decreased above 1400 °C. Positrons annihilated with carbon and silicon core electrons in the matrix increased with decreasing positrons annihilated with silicon vacancies.

In irradiated pure metals, the (S, W) points generally fall on a line segment because only interstitial- and vacancy-type defect clusters are formed during irradiation. Fig. 3 shows the linear relationship between S and W_C below 1200 °C. This indicates that the type of silicon vacancy-related defect responsible for positron trapping is the same after irradiation and annealing up to 1100 °C. However, the (S, W_C) points for samples annealed above 1200 °C were aligned along a different line segment. This suggests that a new type of defects appeared above 1200 °C, which could be the irreversible defects described below and $C_{Si}N_C$ complexes due to the recombination of $V_{Si}N_C$ complexes with carbon split interstitials [21]. In contrast, the relation between S and W_{Si} (Fig. 4) was more complex. The S–W_{Si} plot can be divided into three separate line segments. The first segment is from RT to 1100 °C, where the mobility of silicon vacancies was not prominent. The second is from 1100 °C to 1400 °C, and third is from 1400 °C to 1600 °C. New types of defects are formed during annealing from 1100 °C to 1600 °C. Presumably, irreversible defects, such as anti-defects, were formed during the recovery of $V_{Si}V_C$ di-vacancies from 1100 °C to 1400 °C. The V_C sites of the $V_{Si}V_C$ di-vacancy were replaced by silicon atoms, not carbon atoms. Another type of defect, the $C_{Si}N_C$ complex, was formed from 1400 °C to 1600 °C.

Furthermore, compared with unirradiated 4H–SiC, W_C and W_{Si} were higher at high temperatures. This indicates that more stable interstitial-type defects of silicon, carbon and silicon carbon complexes were formed during isochronal annealing since no vacancy-type defects were detected in 4H–SiC after annealing at 1600 °C.

4. Conclusion

Positron annihilation spectroscopy was used in this work to investigate the types and recovery processes of defects induced by irradiation. After neutron irradiation up to a dose of $3.2 \times 10^{21}/m^2$ ($E > 1$ MeV) at 20 °C, carbon and silicon vacancies and carbon silicon di-vacancies were formed. The recovery process comprised four stages. More stable $V_{Si}N_C$ complexes were formed in stage III (1100–1400 °C), which dissociated in stage IV (>1400 °C). Vacancy-type defects in 4H–SiC were annealed out at 1600 °C, but interstitial-type defects and anti-site defects were stable. These defects will affect thermal conductivity in fusion systems.

References

[1] S.M. Kang et al., Nucl. Instr. Meth. A 579 (2007) 145.
[2] L.H. Rovner, G.H. Hopkins, Nucl. Technol. 29 (1976) 274.
[3] Th. Lingner et al., Physica B 308–310 (2001) 625.
[4] A. Kawasuso et al., Appl. Phys. Lett. 83 (2003) 3950.
[5] J.A. Freitas et al., J. Appl. Phys. 61 (1987) 2011.
[6] A. Dupasquier, A.P. Mills Jr., Positron Spectroscopy of Solids, IOS, Amsterdam, 1995.
[7] P. Asoka-Kumar, M. Alatalo, V.J. Ghosh, A.C. Kruseman, B. Nielsen, K.G. Lynn, Phys. Rev. Lett. 77 (1996) 2097.
[8] (a) Q. Xu, T. Yoshiie, K. Sato, Phys. Rev. B73 (2006) 134115;
(b) Q. Xu, T. Yoshiie, K. Sato, Philos. Mag. Lett. 87 (2007) 65;
(c) Q. Xu, T. Yoshiie, K. Sato, Philos. Mag. Lett. 88 (2008) 353.
[9] K. Fukumoto et al., J. Nucl. Mater. 373 (2008) 289.
[10] A. Sachdeva et al., Diamond Related Mater. 13 (2004) 1719.
[11] S.L. Wu et al., Acta Phys. Sinica 55 (2006) 6129.
[12] W. Puff, A.G. Balogh, P. Mascher, Mater. Sci. Forum 338–342 (2000) 969.
[13] G. Brauer, W. Anwand, P.G. Coleman, A.P. Knights, F. Plazaola, Y. Pacaud, W. Skorupa, J. Stormer, P. Willutzki, Phys. Rev. B 54 (1996) 3084.

[14] S.B. Orlinski, J. Schmidt, E.N. Mokhov, P.G. Baranov, Phys. Rev. B 67 (2003) 125207.
[15] S. Dannefaer, D. Craigen, D. Kerr, Phys. Rev. B 51 (1995) 1928.
[16] Y. Zhang, W.J. Weber, W. Jiang, C.M. Wang, V. Shutthanandan, A. Hallen, J. Appl. Phys. 95 (2004) 4012.
[17] A. Kawasuso, H. Itoh, T. Ohshima, K. Abe, S. Okada, J. Appl. Phys. 82 (1997) 3232.
[18] F. Gao, W.J. Weber, J. Appl. Phys. 94 (2003) 4348.
[19] H. Itoh, M. Yoshikawa, I. Nashiyama, E. Sakuma, J. Appl. Phys. 66 (1989) 4529.
[20] A.I. Girka, V.A. Kuleshin, A.D. Mokrushin, E.N. Mokhov, S.V. Svirida, A.V. Shishkin, Sov. Phys. Semicond. 23 (1989) 1337.
[21] U. Gerstmann, E. Rauls, Th. Frauenheim, H. Overhof, Phys. Rev. B 67 (2002) 205202.